

## Microstructures and nonstoichiometry in schafarzikite-like minerals

MARCELLO MELLINI

*C.N.R., Centro di Studio per la Geologia Strutturale e Dinamica dell' Appennino  
Via S. Maria 53, 56100, Pisa, Italy*

MARC AMOURIC, ALAIN BARONNET AND GENEVIEVE MERCURIOT

*C.N.R.S., Centre de Recherche sur les Mecanismes de la Croissance Cristalline  
Campus Luminy, Case 913, 13288 Marseille Cedex 2, France*

### Abstract

Versiliaite ( $\text{Fe}_{12}\text{Sb}_{12}\text{O}_{32}\text{S}_2$ , *Pbam*,  $a = 8.492$ ,  $b = 8.326$ ,  $c = 11.938\text{\AA}$ ) and apuanite ( $\text{Fe}_{20}\text{Sb}_{16}\text{O}_{48}\text{S}_4$ ,  $P4_2/mbc$ ,  $a = 8.372$ ,  $c = 17.974\text{\AA}$ ) are closely related to schafarzikite ( $\text{Fe}_4\text{Sb}_8\text{O}_{16}$ ,  $P4_2/mbc$ ,  $a = 8.59$ ,  $c = 5.91\text{\AA}$ ), from which they are derived by sulfide insertion, substitution of  $^{\text{IV}}\text{Fe}^{3+}$  for  $^{\text{III}}\text{Sb}^{3+}$ , and oxidation of  $^{\text{VI}}\text{Fe}^{2+}$  to  $^{\text{VI}}\text{Fe}^{3+}$ .

Transmission electron microscopy shows in apuanite the presence of wide regular regions, scattered faults and regions with a high density of faults. The regular sequence is interrupted by insertion of a phase with  $12\text{\AA}$  periodicity (versiliaite). Usually, (001) is the boundary between the two phases, with the guest phase lamellae typically up to twelve  $c$  periods thick. Less frequently, phase boundaries lying in planes normal to (001) have also been recorded, e.g., a (001) lamella,  $36\text{\AA}$  thick, is crossed by a (110) boundary plane normal to the lamella plane; whereas a  $2 \times 18\text{\AA}$  thick apuanite region occurs on one side of the boundary, a  $3 \times 12\text{\AA}$  thick versiliaite region is present on the other side. The crystals of versiliaite are characterized by large grain domain structure. Wide domains of versiliaite are mixed with wide domains of schafarzikite. The results of this study, which confirm the presence of sulfur-poor phases inside both apuanite and versiliaite, lead to an understanding of the nonstoichiometry in this mineral group in terms of microstructures.

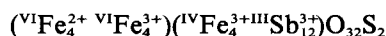
### Introduction

The structural and chemical relationships among the minerals of the schafarzikite group have been summarized by Mellini, Merlino and Orlandi (1979) and by Mellini and Merlino (1979). Relevant crystallographic and chemical data are reported in Table 1.

Schafarzikite,  $\text{FeSb}_2\text{O}_4$ , is the parent phase. The crystal structure (Fischer and Pertlik, 1975) is characterized by columns of edge-sharing  $\text{Fe}^{2+}$  octahedra, connected by corner sharing to parallel chains of  $\text{Sb}^{3+}$   $\psi$ -tetrahedra (trigonal pyramids with an electron lone pair as fourth ligand).

Versiliaite and apuanite can be conveniently described as both stuffed and substitutional derivative structures. The idealized derivation mechanism requires the insertion of a sulfide anion among two  $\psi$ -tetrahedral sites, the substitution in these two sites of  $^{\text{IV}}\text{Fe}^{3+}$  for  $^{\text{III}}\text{Sb}^{3+}$  and charge balance by oxidation of two octahedral  $\text{Fe}^{2+}$  ions to  $\text{Fe}^{3+}$ . Insertion of a sul-

fide anion every fourth  $\psi$ -tetrahedral cation leads to versiliaite, with



as ideal unit cell content, orthorhombic symmetry and  $c$  parameter being twice that of schafarzikite.

The insertion of a sulfide anion every third  $\psi$ -tetrahedral cation leads to apuanite, with



as ideal unit cell content,  $c$  parameter three times the corresponding one of schafarzikite, and space group the same as in the parent phase. Following this scheme, Mellini and Merlino (1979) hypothesized other possible phases and proposed a comprehensive crystal chemical formula for the whole group.

All the derivative structures are characterized by cross-linking of the  $\psi$ -tetrahedral chains. These units polymerize to build up double chain ribbons (if the

Table 1. Relevant data for schafarzikite-like minerals

Schafarzikite		$a = 8.59, c = 5.91 \text{ \AA}, \text{ space group } P4_2/mbc$
a)	$VI_{Fe_4}^{2+} III_{Sb_8}^{3+} O_{16}$	
b)	$(Fe_{3.54}^{2+} Zn_{0.20}^{2+}) (Sb_{6.75}^{3+} As_{1.42}^{3+}) O_{16}$	
Versiliaite		$a = 8.492, b = 8.326, c = 11.938 \text{ \AA}, Pbam$
a)	$(VI_{Fe_4}^{2+} VI_{Fe_4}^{3+}) (IV_{Fe_4}^{3+} III_{Sb_{12}}^{3+}) O_{32} S_2$	
b)	$(Fe_{4.65}^{2+} Zn_{1.04}^{2+} Fe_{2.43}^{3+}) (Fe_{2.90}^{3+} Sb_{11.76}^{3+} As_{1.34}^{3+}) O_{32} S_{1.33}$	
Apuanite		$a = 8.372, c = 17.974 \text{ \AA}, P4_2/mbc$
a)	$(VI_{Fe_4}^{2+} VI_{Fe_8}^{3+}) (IV_{Fe_8}^{3+} III_{Sb_{16}}^{3+}) O_{48} S_4$	
b)	$(Fe_{4.15}^{2+} Zn_{0.32}^{2+} Fe_{7.40}^{3+}) (Fe_{6.87}^{3+} Sb_{15.64}^{3+} As_{1.49}^{3+}) O_{48} S_{3.57}$	
a) ideal unit cell content; b) actual unit cell content		

insertion is every  $2n \psi$ -tetrahedra) or interlaced sheets (if the insertion is every  $2n + 1 \psi$ -tetrahedra). For instance, Figure 1a shows the crystal structure of apuanite, in terms of octahedral columns and  $\psi$ -tetrahedral chains. Figure 1b shows the  $\psi$ -tetrahedral sheet present in apuanite. A schematic view of the crystal structure, described in terms of chains, double chain ribbons and sheets, is given in Figure 2.

Many data support the hypothesis of the presence

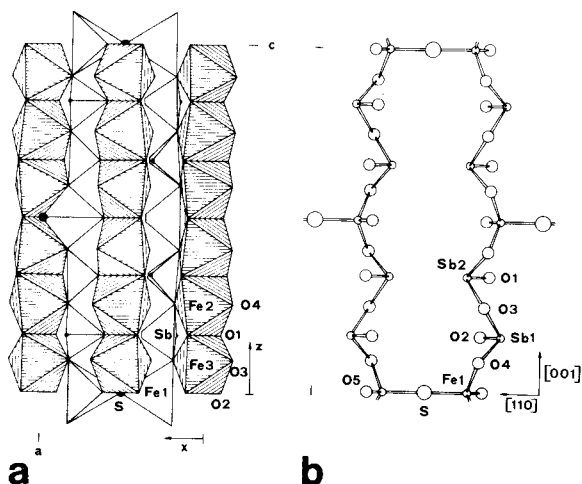


Fig. 1. a) Crystal structure of apuanite, as seen along [010]; b)  $\psi$ -tetrahedral sheet of apuanite, as seen along [110].

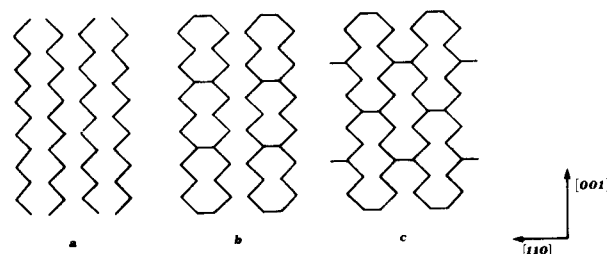


Fig. 2. Schematic drawings of the crystal structures, as seen along [110]: a) single chains of schafarzikite; b) double chain ribbons of versiliaite; c) infinite sheet of apuanite.

of structural disorder. In fact, systematic deviations from the stoichiometric composition were observed by repeated electron microprobe analyses (Table 1). These figures were in agreement with the significant partial occupancies obtained during the X-ray structure refinement, leading Mellini and Merlino (1979) to postulate the presence of structure domains.

Using transmission electron microscopy, we have achieved a better understanding of the previous chemical and structural data, in terms of the real structures of these phases. The purpose of this study is to verify the hypothesis of defect structures, understand the nature of the defects, and investigate the existence, at least in small domains, of other yet unknown phases.

### Experimental

The crystals used in this study come from the specimens described by Mellini, Merlino and Orlandi (1979). Electron transparent foils were prepared by wet grinding and dispersion on carbon coated grids. As (110) is the most prominent cleavage, the fragments are mainly (110) flakes.

The images were obtained by a JEOL 100C electron microscope, equipped with an objective lens characterized by  $C_s = 1.6 \text{ mm}$ , hairpin filament and no tilting facility. No relevant radiation damage was observed. An objective aperture was selected to collect diffracted beams corresponding to direct spacings greater than  $3.0 \text{ \AA}$ . Typically, the most informative contrast was obtained at  $800\text{--}1200 \text{ \AA}$  underfocus, assuming as zero the least contrast focus on the carbon film.

The study was based mainly on monodimensionally resolved images, although occasional bidimensional images were also recorded. Previous calculations of the charge density, as projected along the directions of observation, show no relevant bidimensional contrast. This is obviously due to the absence of features like tunnels or overlapping heavy

atoms. The simulated images, calculated using the SHRLI program (O'Keefe and Buseck, 1979), usually do not exhibit relevant bidimensional contrast which can be resolved by our microscope. Therefore, attention was paid to the study of the  $c$  periodicities only, imaged by systematic  $00l$  reflections. No accurate excitation of the outer reciprocal lattice lines is required for recording these images.

### Results

The crystals of apuanite, when imaged to resolve (001) planes, show both regular sequences and faulted regions. The fault density is widely variable, ranging from scattered faults to heavily faulted regions.

As regards the nature of the faults, they can be ascribed to the insertion, into the  $18\text{\AA}$  matrix, of a  $12\text{\AA}$  phase, *i.e.*, versiliaite. This last phase is present as widely extended (001) lamellae, which are a few unit cells thick in the [001] direction.

Figure 3 shows the faulted region inside an otherwise regular large crystal of apuanite. The regular repetition of  $18\text{\AA}$  periods is interrupted by insertion of versiliaite, which forms a (001) lamella ten  $c$  periods thick ( $120\text{\AA}$ ). Such faults, inside the regular apuanite matrix, have been extensively observed. Their thickness is up to  $144\text{\AA}$ , typically ranging from two to six  $c$  periods ( $24$  to  $72\text{\AA}$ ). Figure 4 is an image of a heavily faulted crystal. Several lamellae of versiliaite and apuanite alternate along [001]. Owing to the orientation, [110], and systematic extinctions,  $hhl$  present for  $l = 2n$ , the lattice fringes corresponding to apuanite regions are characterized by the halved  $9\text{\AA}$  period. No superstructure involving ordered combination of apuanite and versiliaite lamellae has been recorded.

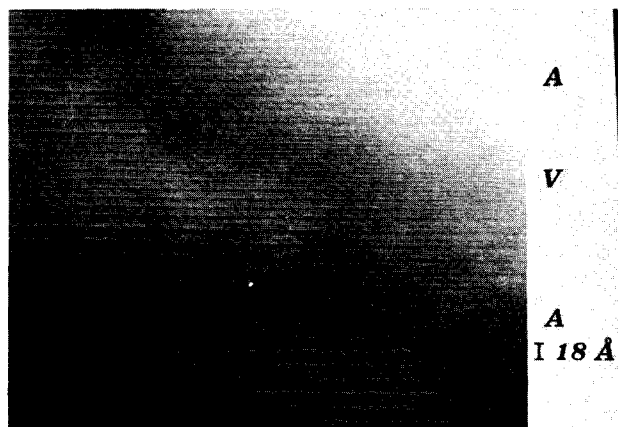


Fig. 3. (001) versiliaite lamella inside a regular matrix of apuanite.



Fig. 4. Heavily disordered sequence of versiliaite ( $12\text{\AA}$  lattice fringes) and apuanite ( $9\text{\AA}$  lattice fringes) lamellae.

The structural relationship between (001) lamellae of versiliaite and apuanite is given in Figure 5, in terms of double chain ribbons and sheets. As shown, the main structural features are preserved through the whole crystal, namely  $\psi$ -tetrahedral chains and the related octahedral columns (not shown in Fig. 5). At the level of the fault, the polymerization of the chains by sulfur bridges changes. The continuous sheet of apuanite becomes locally an array of double chain ribbons, due to the lower insertion of sulfide atoms.

So far we have described wide (001) versiliaite lamellae, which extend through the whole crystal fragment characterized by the apuanite structure. Additionally, laterally terminated lamellae have been occasionally recorded. One of them present in Figure 4 is enlarged in Figure 6, which also gives a schematic drawing of the lattice fringe arrangement and

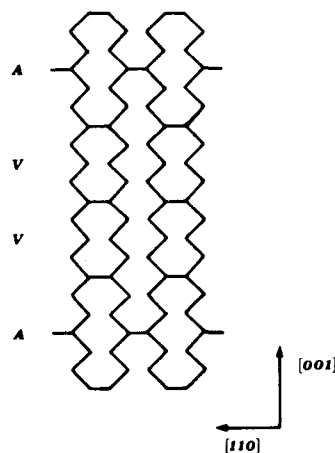


Fig. 5. Structural arrangement in crystals of apuanite faulted by (001) lamellae of versiliaite.

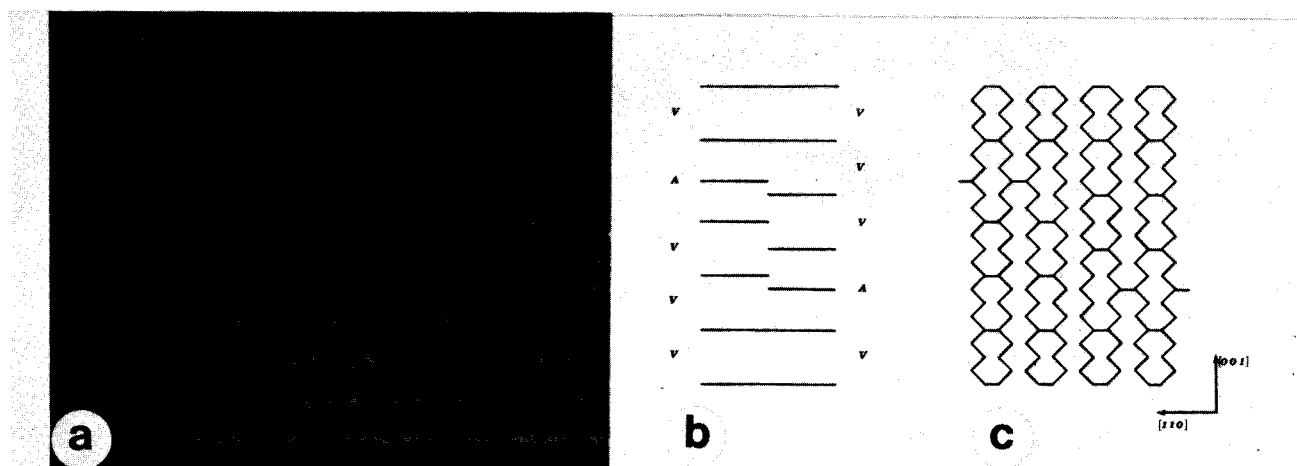


Fig. 6. a) lattice image of a crystal of apuanite (9Å fringes) faulted by a laterally interrupted lamella of versiliaite; b) sketch showing the lattice fringe arrangement; c) proposed interpretation of the structural arrangement.

the corresponding structural interpretation. A severe problem in electron microscopy is the amount of shift of the image with respect to the structure, when we depart from the optimum structure imaging conditions. Notwithstanding this difficulty, a geometric pattern of sulfur atoms (001) planes can be drawn. In the case of versiliaite, the pattern shows the same 12Å spacing as the (001) lattice fringes. On the other hand, the apuanite sulfur pattern is characterized by the 9Å spacing, which corresponds to the spacing of (002) lattice fringes. Therefore, in spite of any possible shift of the image with respect to the structure, the sulfur arrangement can be inferred from the lattice fringes.

A similar, perhaps more complex case, is shown in Figure 7. Once more, a matrix of apuanite, producing 9Å fringes, is crossed by three versiliaite lamellae. Whereas on the right side of the figure these lamellae are  $5 \times 12$ ,  $2 \times 12$  and  $5 \times 12$ Å thick respectively, on



Fig. 7. Laterally interrupted lamellae of versiliaite inside apuanite.

the other side they extend  $2 \times 12$ ,  $2 \times 12$  and  $2 \times 12$ Å, respectively. The structural arrangement can be easily deduced using the same scheme as in Figure 6.

Such lateral phase contacts are characterized by a close relation between the numbers of the unit cells involved. So, in the case of Figure 7, a deficit of six unit cells of versiliaite ( $6 \times 12 = 72$ Å) is balanced by four unit cells of apuanite ( $4 \times 18 = 72$ Å).

Another kind of fault, recorded at least twice for apuanite, is shown in Figure 8. A regular sequence of 18Å fringes is crossed by two groups of four aligned strain contrast blobs, these two groups being colinear and parallel to the [001] direction (Fig. 8a). The contrast is also symmetric with respect to [001]. In Figure 8b, we notice that an extra plane of apuanite is present in the lower part of the micrograph when compared to the upper part. Therefore, the Burgers circuit around each contrast group indicates an 18Å component, along [001], of the fault vector. This strongly suggests that each contrast group results from a unit dislocation. The unit dislocation is dissociated into four partial dislocations, which are seen on end, confined in a ribbon-like region. Going from outside to inside the ribbon along [001], we notice first a bending and then a 9Å shift of the 18Å lattice fringes. This 9Å shift not only disturbs the sulfur bridge configuration, but also the tetrahedral-octahedral pattern across the fault plane. This should imply a high fault energy which, combined with heavy strain contrasts, suggests an extrinsic origin of the fault. It is likely that the fault originated during the grinding process, rather than during crystal growth.

For versiliaite, repeated preparations of micro-

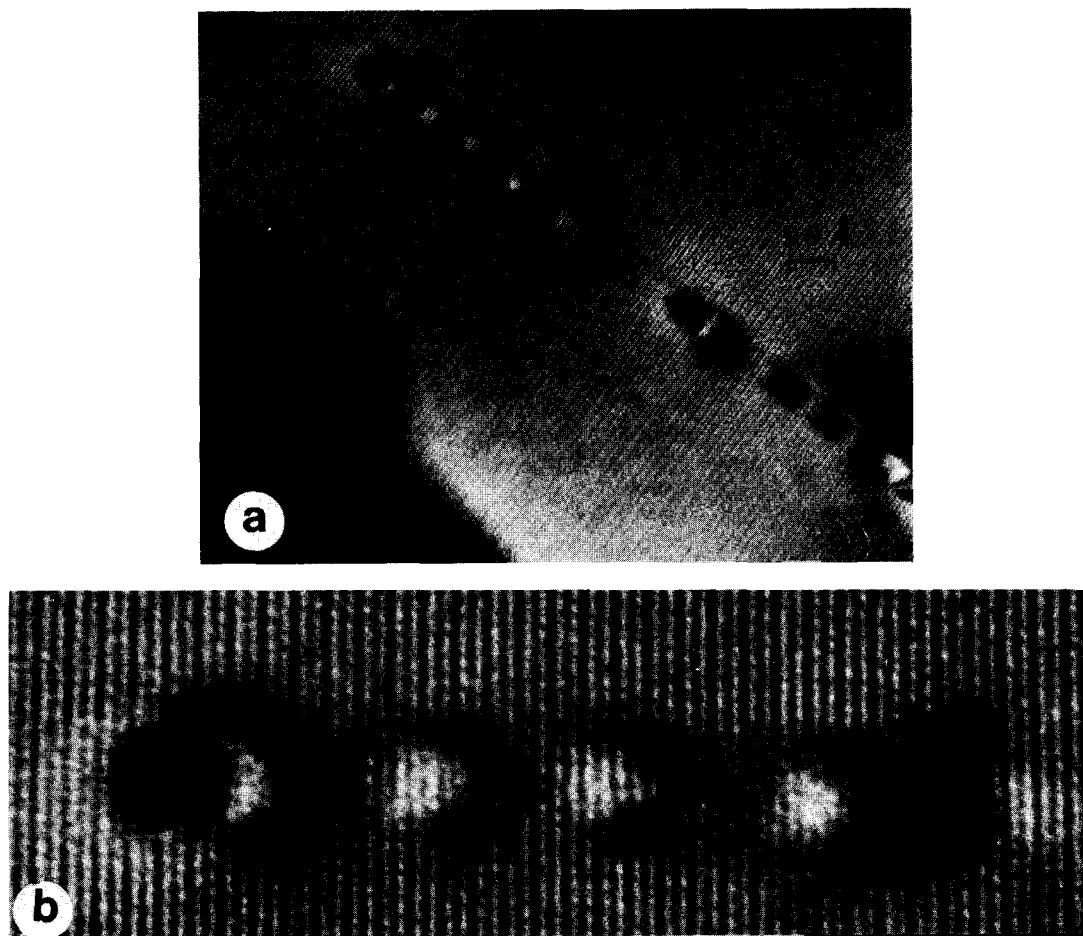


Fig. 8. a) Dislocation contrast in apuanite; b) enlarged portion.

scope grids, by carefully grinding a few tiny crystals picked up from different specimens, always led to very regular fragments, with no faults at all. The fragments always belonged to two different mineral phases, versiliaite itself and schafarzikite. It was possible to study a large transparent foil, about  $2000 \times 3500 \text{ \AA}$  wide, showing the presence of three different domains: a large central region with  $6 \text{ \AA}$  periodicity, a slightly smaller triangular slab with  $12 \text{ \AA}$  periodicity (its side is about  $1500 \text{ \AA}$  long) and another smaller  $12 \text{ \AA}$  region. The boundaries between the various domains are shown in Figure 9. Inside each domain several unit cells are regularly stacked one upon the other, along  $[001]$ . Various domains alternate along  $[110]$ . No sharp boundary seems to exist.

The interpretation of Figure 9 was supported by selected area diffraction, which showed the two  $[110]$  reciprocal lattices of versiliaite and schafarzikite. Moreover, another argument excludes the possibility that the two different periodicities may be due to en-

hancement of dynamic effects as the crystal thickness increases. Indeed, the fringe period does not change with increasing crystal thickness, from the edge to the center, but rather along the edge of the crystal.

Schafarzikite, like versiliaite, after grinding produces regular fragments belonging to two mineral phases, schafarzikite itself and, less frequently, versiliaite. We conclude therefore that both versiliaite and schafarzikite are characterized by a large grain domain structure, consisting of fault-free domains of versiliaite and schafarzikite. Furthermore, it is possible that the small crystal fragments produced by grinding are the result of a preferred separation of the two different structures, which break up at the boundary. Such a domain structure is in agreement with that claimed by Mellini, Merlino and Orlandi (1979), for the X-ray powder diffraction pattern of schafarzikite. They observed that this phase was mixed with versiliaite, as revealed by superposition of the two patterns.

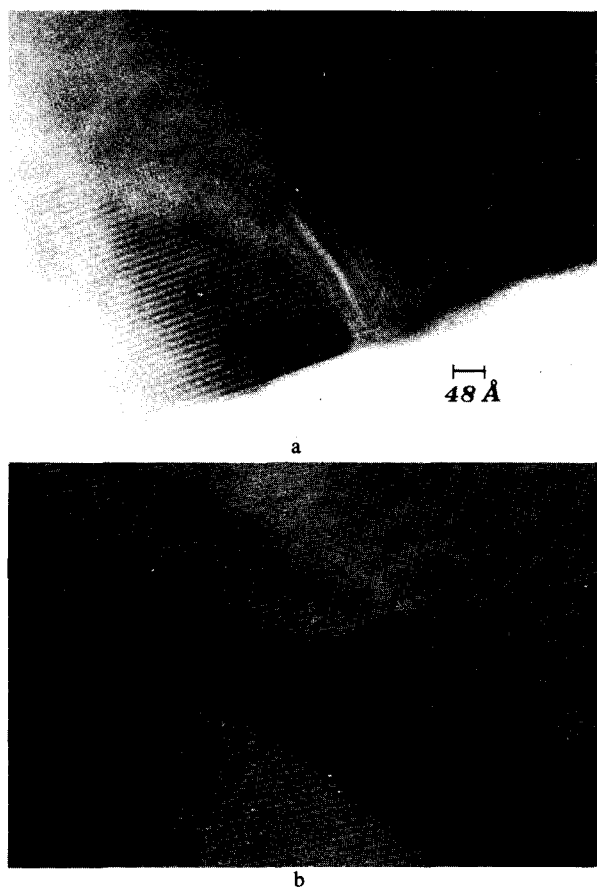


Fig. 9. Boundaries between versiliaite and schafarzikite domains.

#### Discussion on nonstoichiometry

As previously discussed, chemical as well as structural data show significant partial occupancy for sulfide ions, both in versiliaite and apuanite. This is in agreement with the related incomplete substitution of  $^{IV}\text{Fe}^{3+}$  for  $^{III}\text{Sb}^{3+}$ . A qualitative understanding of this feature is easily achieved by taking into account the microstructure as observed by TEM. Indeed, both apuanite and versiliaite are intergrown with sulfur poorer phases, versiliaite and schafarzikite respectively. This feature obviously leads to sulfur content lower than the ideal, stoichiometric values (Table 1).

However, the quantitative interpretation is not straightforward and requires comment. The chemical data reported by Mellini, Merlino and Orlandi (1979) were gathered on crystal fragments previously tested by X-ray diffraction techniques (namely Weissenberg and precession photographs). In this step, no caution was taken to carefully measure the intensity of the spots. As usual, symmetry and periodicities of the reciprocal lattice were studied. In this case, crystal frag-

ments in which a versiliaite matrix is intergrown in parallel association with schafarzikite domains may be labelled versiliaite. Indeed, all the reciprocal lattice points of schafarzikite superpose with the reciprocal lattice points of versiliaite having  $l = 2n$ . The small differences in the values of the  $a^*$  and  $b^*$  parameters cause a broadening of the diffraction spots. In fact, the scan width used in intensity data collection for versiliaite and apuanite was rather large,  $2.20$  and  $2.00^\circ$  respectively.

On the other hand, crystal fragments where a schafarzikite matrix is intergrown with versiliaite domains may be labelled schafarzikite only if the versiliaite domains are not so widely developed to produce a characteristic X-ray diffraction pattern. Therefore, the presence of a common subcell results in the selection of crystals of schafarzikite with the least content of versiliaite domains and in the selection of crystals of versiliaite with a random content of schafarzikite domains.

For apuanite, which is faulted by insertion of versiliaite lamellae, the two reciprocal lattices do not overlap. But, as the fault density is low and the thickness of the versiliaite lamellae is always thinner than  $200\text{\AA}$ , these lamellae do not produce an observable X-ray diffraction pattern.

We can therefore explain the close correspondence between the actual and the ideal crystal chemical formula of schafarzikite. Indeed, notwithstanding the domain structure, the fragment used in microprobe analysis was evidently characterized by the least development of versiliaite domains.

For versiliaite, chemical as well as structural data indicate the presence of nearly 1.5 sulfur atoms per unit cell, whereas the ideal value is 2.0. This requires that the analyzed fragment is characterized by a domain structure with 75 percent versiliaite and 25 percent schafarzikite volumes, owing to the presence of two sulfur atoms per unit cell in versiliaite and the absence of sulfur in schafarzikite. Such a ratio is in agreement with the frequency of observation of schafarzikite domains together with versiliaite domains, thus arguing for a stoichiometric composition of each component phase.

Apuanite is characterized by an actual content of 3.5 sulfur atoms per unit cell, whereas 4.0 is the ideal value. As a volume of versiliaite corresponding to the unit cell of apuanite ideally contains 3.0 sulfur atoms, similar quantities of the two intergrown phases, namely apuanite and versiliaite, would be required to explain such a figure in the chemical analysis. This is not supported by the TEM observations.

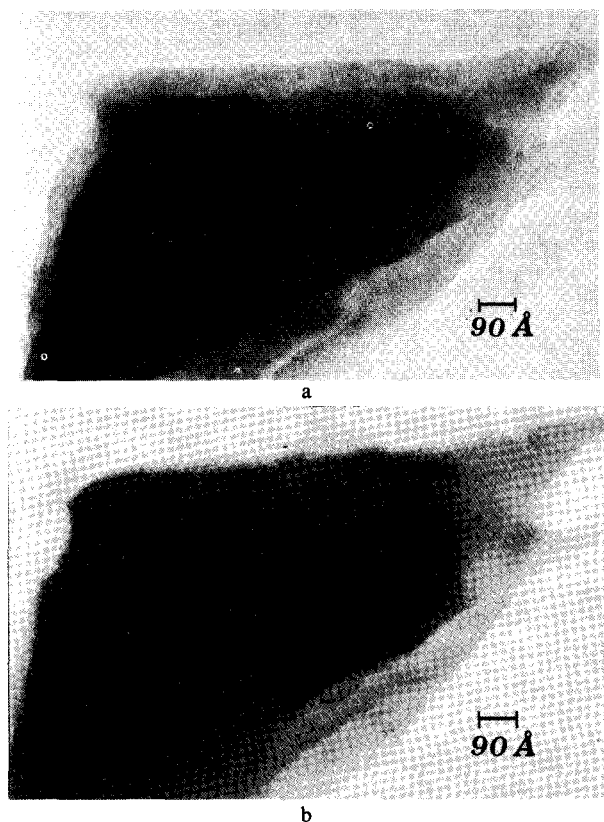


Fig. 10. Faulted crystal of apuanite: a) image at nearly 1200Å underfocus showing 9Å periodicity; b) image at nearly focus showing 18Å periodicity.

Indeed, the amount of versiliaite lamellae inside apuanite is well below 50 percent, at least an order of magnitude smaller. Assuming that the chemical and structural data are correct and that no 12Å phase different from versiliaite may occur, the most likely explanation would lie in the existence of another, sulfur poor, 18Å phase. Nonstoichiometric behavior, involving extensive sulfur vacancies, can indeed be ruled out by analogy with the previously argued stoichiometric composition of each component phase in the versiliaite-schafarzikite assemblages. Such an 18Å phase has been hypothesized by Mellini and Merlino (1979), who identified it by the sequence (0,1,2,3,4,5),6. It has unit cell parameters  $a \approx b \approx 8.4$ ,  $c \approx 18\text{Å}$ , space group  $Pbam$ , ideal crystal chemical formula



The presence in apuanite of 20 percent of this phase would explain the chemical and structural data.

Unfortunately, such a phase cannot be easily distinguished from apuanite by electron microscopy. In fact, it is expected to produce similar 18Å fringes and to differ from apuanite by the presence of reflections  $hhl$  with  $l$  odd (thus producing 18Å fringes also in [110] orientation). Actually, we have frequently observed these spots, in regions with both the 18 and 9Å periodicities. It is not known whether these spots and the corresponding periods of the lattice fringes are due to the coexistence of the two phases, to dynamic diffraction effects, or to imaging conditions (e.g., multiple diffraction, amount of defocus or thickness of the crystal). For instance, Figure 10 shows a faulted crystal of apuanite, observed along [110]. Whereas the image recorded at nearly 1200Å underfocus shows 9Å fringes, a nearly focused image exhibits 18Å fringes.

Most probably, further X-ray and electron microprobe studies would be necessary to demonstrate the existence of this postulated phase. The goal would be to find crystals with 18Å periodicity, significant deviation from the tetragonal  $4/mmm$  Laue symmetry, presence of reflections  $hhl$  with  $l = 2n + 1$ , as well as a sulfur content approaching two atoms per unit cell.

### Acknowledgments

M.M. wishes to thank Professor R. Kern and the staff of the Centre de Recherche sur les Mécanismes de la Croissance Cristalline, for the scientific and technical help and for the friendly reception he received during his stay in Marseille.

### References

- Fischer, R. and Pertlik, F. (1975) Verfeinerung der Kristallstruktur des Schafarzikits,  $\text{FeSb}_2\text{O}_4$ . *Tschermaks Mineralogische und Petrographische Mitteilungen*, 22, 236–241.
- Mellini, M., Merlino, S. and Orlandi, P. (1979) Versiliaite and apuanite, two new minerals from the Apuan Alps, Italy. *American Mineralogist*, 64, 1230–1234.
- Mellini, M. and Merlino, S. (1979) Versiliaite and apuanite: derivative structures related to schafarzikite. *American Mineralogist*, 64, 1235–1242.
- O'Keefe, M. A. and Buseck, P. R. (1979) Computation of high resolution TEM images of minerals. *Transactions of the American Crystallographic Association*, 15, 27–44.

Manuscript received, September 24, 1980;  
accepted for publication, April 28, 1981.